Kazimierz J. PLUCIŃSKI

Electronics Department, Military University of Technology
ORCID: https://orcid.org/0000-0001-9353-3786

doi:10.15199/48.2023.12.12

Notes on the interpretation of conductivity measurement results of GST-based PCM structures in reset state with respect to the origin of conductivity drift

Abstract: *The conductivity drift of GST ($Ge_2Sb_2Te_5$)-based PCM (Phase Change Memory) structures in the reset state hinders the development of multi-level PCM memories and their applications. Despite intensive research, the origin of this drift remains unclear. The results presented here of analysis, based on the JMAK and Maxwell-Wagner models, indicate that the current interpretation of the results of conductivity measurements of GST-based PCM structures in the reset state may cause ambiguity in determining the origin of the conductivity drift of these structures in this state.*

Streszczenie*: Dryf konduktywności struktur pamięci zmiennofazowych (PCM--Phase Change Memory) formowanych na bazie GST ($Ge_2Sb_2Te_5$) w stanie reset utrudnia rozwój wielopoziomowych pamięci PCM i ich zastosowań. Pomimo intensywnych badań pochodzenie tego dryfu pozostaje niejasne. Przedstawione wyniki analizy na przykładzie modeli JMAK i Maxwella-Wagnera wskazują, że aktualna interpretacja wyników pomiarów konduktywności tych struktur może przyczyniać się do niejednoznaczności w określaniu pochodzenia dryfu ich konduktywności w tym stanie.*
(Uwagi dotyczące interpretacji wyników pomiarów konduktywności struktur PCM na bazie GST w stanie reset w odniesieniu do pochodzenia dryfu konduktywności)

Słowa kluczowe: *dryf konduktywności, chalkogenki, materiały Ge-Sb-Te, pamięć zmiennofazowa*
Keywords*: conductivity drift, chalcogenides, Ge-Sb-Te materials, phase-change memory*

Introduction

The "working" element of the *PCM* devices is the small volume of a phase change material *(PCM)* contained between the two electrodes [e.g.,1]. A certain proportion of this material is electrically switched between a crystalline state ("set state" – with high conductivity) and an amorphous state ("reset state" – with low conductivity). *GST* ($Ge_2Sb_2Te_5$) is one of the basic, most commonly used and most comprehensively tested phase change materials among the compositions along the Sb_2Te_3-*GeTe* tie-line [e.g., 2,3]. Of the three known *GST* phases - stable hexagonal phase, metastable cubic phase, and amorphous phase - the change between the metastable crystalline (set) and amorphous (reset) states is employed since the phase change between the two phases can take place in nanoseconds [4]. The basic requirements for the use of this material in *PCM* memory include conductivity stability in both reset and set states.

While in the set (crystalline) state this material is conductively stable, in the reset state two intervals can be distinguished with respect to dependence of the conductivity over time [1,2,3,5]:

1^0 - after switching to the reset state, the conductivity decreases as a function of time - this phenomenon is called the conductivity drift (or resistivity drift) – Fig.1.

2^0 - after some time, as the crystallization of the amorphous fraction progresses, the percolative threshold is attained and conductivity begins to increase rapidly (or resistivity begins to decrease rapidly [e.g., 2, Fig. 5.2]).

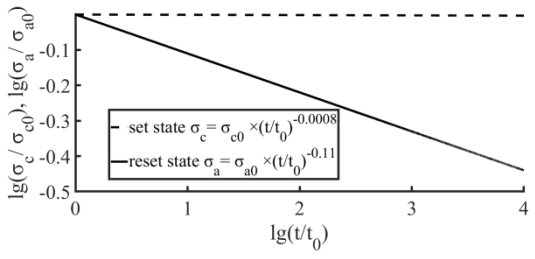

Fig. 1. Typical conductivity of *a-GST* (reset state) and *c-GST* (set state) versus time in lg-lg scale based on the reported [e.g., in 6] drift exponent for crystalline *c-GST* in the set state (-0.0008) and for amorphous *a-GST* in the reset state (-0.11)

This letter concerns research aimed at explaining the origin of the conductivity drift.

The conductivity drift of the *PCM* structures is the subject of very intensive research [e.g., 7 and references ibid] because this phenomenon is crucial for the further development of the *PCM* technology. It stands in the way of benefiting from the basic advantage of the *PCM* memory - the construction of multilevel memory cells and its applications, e.g., in the brain-inspired computing [5,7,8,9].

The key element underlying the concepts of the origin of the drift conductivity of *GST*-based *PCM* structures in the reset state is the observed linear relationship between $ln(\sigma)$ and $ln(t)$ in that state [6,10]:

$$(1) \quad ln\left(\frac{\sigma(t)}{\sigma_0}\right) = ln\left[\left(\frac{t}{t_0}\right)^{-\nu}\right]$$

or equivalently:

$$(2) \quad \sigma = \sigma_0 \left(\frac{t}{t_0}\right)^{-\nu}$$

where σ is the measured conductivity, σ_0 is the conductivity at $t=t_0$ and ν is the so-called conductivity drift exponent representing changes of the $ln[\sigma(t)]$ versus $ln(t)$ according to:

$$(3) \quad \nu = -\frac{d\, ln(\sigma)}{d\, ln(t)}$$

Linearity of the relationship (1) means that $\nu(t)=const$. This slowly decreasing conductivity with time (e.g. for GST $\nu \approx -0.11$ at the reset state, while in the set state $\nu \approx -0.0008$ [6]) fall within the energetic point of view according to which conductivity drift is interpreted as a symptom of a structural transition from a highly stressed glass state, existing after switching to reset state, towards an energetically more favorable ideal glass configuration [5,9,10].

Very different and sometimes opposing mechanisms have been proposed to account for the conductivity drift according to relationships (1,2) [7,11].

These include [11] extrinsic mechanisms, such as structural ageing [e.g., 2,3,6] or mechanical-strain relief

[e.g., 4,12,13], as well as intrinsic electronic mechanisms for which the model was developed in terms of the long-time, deep-trap release and subsequent recombination of charge carriers [11].

However, despite very intensive research, the origin of this phenomenon is far from clarified [2,3,6,7,11,14]. At present these studies can be boiled down to the development of the conductivity models of the *GST* amorphous fraction. Efforts in the field of this modeling go in this direction so that the conductivity drift exponent determined on the base of these models has values as close as possible to the measured values of this drift exponent for *GST*-based *PCM* structures.

However, after switching to the reset state, the crystallization of the amorphous region - formed as the result of this switching - begins, and as a result a composite of *GST* crystallites distributed in an amorphous *GST* matrix is formed and conductivity of such composite is measured.

Thus, conclusions about the nature of drift are drawn by comparing the theoretical results developed for the relaxation phenomena occurring in an amorphous material with the results of measurements of a composite consisting of crystallites immersed in an amorphous matrix.

Expression (1) in fact – concerns the measured dependence of the conductivity on the time for such a composition.

There are many models reported in the literature to describe the conductivity of such a composition [e.g.,15,16,17].

Procedure outline

To illustrate the effect of crystallization of the amorphous *GST* fraction in the reset state on the interpretation of conductivity measurements in this state, the Maxwell – Wagner model of the uniformly distributed spherical elements of one material in the matrix of another material was chosen [16, 17].

In the case under consideration, these are spherical *GST* crystallites uniformly distributed in the amorphous *GST* matrix.

The dc conductivity of such a composition according to this model is defined by the expression [16,17]:

$$(4)\quad \sigma = \sigma_a \frac{2\sigma_a+\sigma_c+2Y(\sigma_c-\sigma_a)}{2\sigma_a+\sigma_c-Y(\sigma_c-\sigma_a)}$$

where σ refers to dc conductivity of the composition, σ_c and σ_a refers to the dc conductivity for crystalline and amorphous fractions respectively and Y refers to volume of the transformed fraction.

Expression (4) could be written in the form of equation for σ_a:

$$(5)\quad A\sigma_a^2 + B\sigma_a + C = 0$$

where:

$$(6)\quad A = 2(1-Y)$$

$$(7)\quad B = \sigma_c(1+2Y) - \sigma(2+Y)$$

$$(8)\quad C = \sigma_c\sigma(Y-1)$$

There are two solutions to equation (5):

$$(9)\quad \sigma_{a1} = \frac{-B+\sqrt{B^2-4AC}}{2A}$$

$$(9a)\quad \sigma_{a2} = \frac{-B-\sqrt{B^2-4AC}}{2A}$$

Only σ_{a1} is physically consisted with the model described by expression (4) according to which $\sigma_{a1} = \sigma$ for $Y = 0$ and $\sigma_{a1} \rightarrow 0$ for $Y \rightarrow 1$, while $\sigma_{a2} = -\sigma_c/2$ for $Y = 0$ and $\sigma_{a2} \rightarrow -\infty$ for $Y \rightarrow 1$.

The final forms of the time dependency of that conductivity will depend on the selection of the function $Y(t)$ representing the time evolution of the volume of the crystallized fraction.

The *JMAK* (Johnson-Mehl-Avrami-Kolmogorov) model [17 - 21 and references ibid] was chosen to illustrate the effect of crystallization on the interpretation of conductivity measurements in the reset state concerning the conductivity drift. Although since its introduction at the turn of 1930/40 many of its improvements, often very sophisticated, have appeared, its original form is still the basis of laboratory practice [20].

For example, as stated in [21]: "*JMAK* kinetics is a fairly good approximation even when the systems depart from its strict requirements and different kinetic approaches lead to similar equations to *JMAK* one".

The *JMAK* equation is a benchmark for verifying various approaches aimed at improving the *JMAK* model.

In that model, the function $Y(t)$ for overall rate of transformation, without isolating nucleation and growth stages and under isothermal annealing conditions is described by the equation [18,19]:

$$(10)\quad Y(t) = 1 - e^{-(kt)^n}$$

or equivalently:

$$(10a)\quad ln\left(ln\left(\frac{1}{1-Y}\right)\right) = n\,ln(t) + n\,ln(k)$$

where t is time, n is the Avrami coefficient, and $k(T)$ is a temperature-dependent effective overall reaction rate, expressed as:

$$(11)\quad k(T) = \nu_f\, exp\left(-\frac{E_A}{k_B T}\right)$$

where E_A is the activation energy of the crystallization, ν_f is the frequency factor, k_B – Boltzmann constant, and T – temperature in *[K]*.

From (10, 10a) it follows that the plot of $ln\,(ln\,(1/(1-Y)))$ as a function of $ln\,(t)$ should be linear with a slope defined by the Avrami coefficient n - Fig. 2.

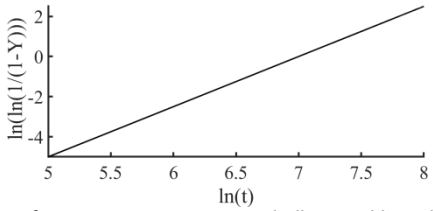

Fig. 2. Plot of $ln\,(ln\,(1/(1-Y)))$ *vs* $ln\,(t)$ is linear with a slope defined by the Avrami coefficient n (for the presented example graph $n=2.5$)

Neither the *JMAK* model, nor the Maxwell-Wagner model take into account percolation phenomena [e.g., 17,22]. Thus, these models can be used for small values of the function $Y\,(t)$. The $Y(t)$-range of the conductivity drift is also limited by percolation phenomena.

There is a huge dispersion of parameters of the *JMAK* model for the *GST*-based *PCM* structures published by leading laboratories, e.g., according to [18]: activation energy values E_A reported in the literature covers a wide spectrum from 0.81 to 3 eV, Avrami coefficient n varies between 1 and 5.8 and the reported values of the frequency factor ν_f varies between 10^{17} and 10^{86} s^{-1}.

Presented in the following results of example calculations were made for: E_A=2 eV and v_f=1.5x10^{22}s^{-1}.

Like in the case of drift exponent ν of the $\sigma(t)$, the following coefficient ν_{a1} representing the change in the $ln[\sigma_{a1}(t)]$ *vs* $ln(t)$, i.e., the drift exponent of the conductivity $\sigma_{a1}(t)$, is introduced:

$$(12)\quad \nu_{a1}(t) = -\frac{d[ln(\sigma_{a1})]}{d[ln(t)]} = -\frac{\sigma'_{a1}}{\sigma_{a1}}t$$

where, considering expression (9) for σ_{a1} and expression (10) for $Y(t)$:

$$(13)\quad \sigma'_{a1} = \frac{d\sigma_{a1}}{dt} = \frac{\{-B'+(2A\sigma_{a1}+B)^{-1}[BB'-2(CA'+AC')]\}-2A'\sigma_{a1}}{2A}$$

$$(14)\quad A' = \frac{dA}{dt} = -2Y'$$

$$(15)\quad B' = \frac{dB}{dt} = Y'(2\sigma_c - \sigma) - \sigma'(Y+2)$$

$$(16)\quad C' = \frac{dC}{dt} = \sigma'\sigma_c(Y-1) - \sigma_c\sigma Y'$$

$$(17)\quad \sigma' = \frac{d\sigma}{dt} = -\nu\sigma_0 t_0^{\nu} k^{\nu+1}\left(ln\frac{1}{1-Y}\right)^{-\frac{1+\nu}{n}}$$

$$(18)\quad Y' = \frac{dY}{dt} = nk(1-Y)[\ln(\frac{1}{1-Y})]^{\frac{n-1}{n}}$$

Calculation results

In Figs 3-5 selected results of the calculations are presented, which illustrate the changes in the conductivity σ_{a1} and its drift ν_{a1} of the amorphous fraction of the composite versus the function $Y(t)$ representing the volume of the transformed fraction. They are calculated under assumption that composition conductivity $\sigma(t)$ changes according to the expression (2) with a constant-time value of the drift exponent ν changing with temperature according to the relation [23]:

$$(19)\quad \nu = 2.5\times10^{-4}\times\frac{T}{\left(1-\frac{T}{760}\right)}$$

where T is the temperature in $[K]$.

It is assumed that the conductivity of the crystalline fraction σ_c does not change with time – as is illustrated in Fig.1. These figures show the calculation results for the frame of time in which $Y(t)$<0.3 – i.e., below the percolation threshold [22], which is assumed to be for $Y(t)$>0.4 [e.g., 24,25].

As already mentioned, the origin of the conductivity drift of *GST*-based *PCM* structures is determined based on the conductivity models of the amorphous *GST* fraction, assuming that this conductivity changes with time according to (1) with a constant value of the drift exponent ν at specified intervals [7].

1.

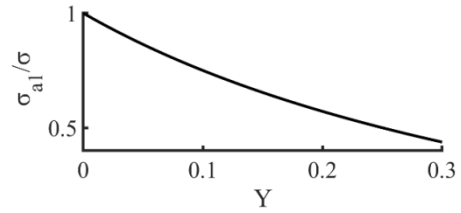

Fig. 3. Ratio σ_{a1}/σ versus volume of the transformed fraction $Y(t)$, for $\sigma=\sigma_0(t/t_0)^{-\nu}$, $\sigma_0=5x10^{-2}$ $[\Omega cm]^{-1}$[2], σ_{c0}=58,5 $[\Omega cm]^{-1}$ [2], $\sigma_c=\sigma_{c0}(t/t_0)^{-0.0008}$, E_A=2eV, n=2.5, $\nu=2.5\times10^{-4}\times T/(1-T/760)$ [23], $\nu_f=1.5x10^{22}$, and T=353 K

However, the results of calculations based on the Maxwell-Wagner and *JMAK* models, presented in Figures 3-5, confirm that linear dependence of $ln(\sigma)$ *vs* $ln(t)$, i.e., with constant drift exponent ν, determined from conductivity measurements of the *GST*-based *PCM* structure in the reset state is ensured under the following circumstances:

with an increase in the volume of the transformed fraction $Y(t)$ the conductivity σ_{a1} of the amorphous fraction of this composition should decrease in relation to the conductivity of the composition σ – Fig.3, e.g., in presented calculations $\sigma_{a1}=\sigma$ for $Y(t)$=0, $\sigma_{a1}=0.97\sigma$ for $Y(t)$=0.01, $\sigma_{a1}=0.75\sigma$ for $Y(t)$=0.1 and $\sigma_{a1}=0.4375\sigma$ for $Y(t)$=0.3.

2. with an increase in $Y(t)$, the drift exponent ν_{a1} of the amorphous fraction conductivity σ_{a1} of this composite should increase in relation to the constant drift exponent ν of the conductivity of the composite – Fig. 5.

So, the ratio ν_{a1}/ν increases with the increase of Y and n, where:

- these increments are linear as a function of n;
- these increments are non-linear as a function of Y - the slope of this relation decreases with the increase in Y.

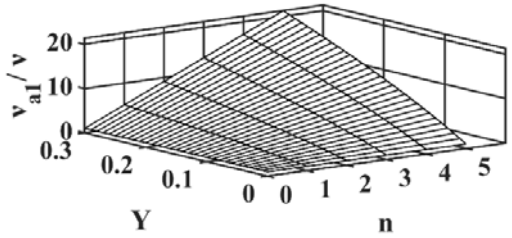

Fig. 4. Ratio of the ν_{a1}/ν versus volume of the transformed fraction $Y(t)$ and Avrami coefficient n. Calculations were carried out for the parameters specified in the description of Fig. 3

The graphs presented in Fig. 4 show that in terms of changes in n in the range (0-5) and Y in the range (0-0.3), ν_{a1}/ν changes in the range from 1 (for n=0; Y=0) to 21.29 (for n=5; Y=0.3), i.e., more than 20 times.

Changes in the ratio ν_{a1}/ν in relation to change of crystallization progress represented by $Y(t)$, i.e., $d(\nu_{a1}/\nu)/dY$ are illustrated in Fig. 5 in the form of a 2-dimensional graph of $d(\nu_{a1}/\nu)/dY$ versus n and Y.

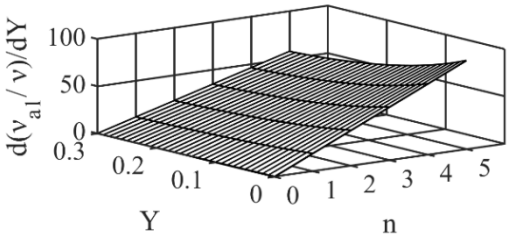

Fig. 5. The rate of change of ν_{a1}/ν as a function of Y and the Avrami coefficient n. Calculations were carried out for the parameters specified in the description of Fig. 3

The rate of change $d(\nu_{a1}/\nu)/dY$ increases from 0 (for n=0 and Y=0.3) to over 90 (for n=5 and Y=0). The rate of these changes increases linearly as a function of the increase in Avrami coefficient n and decreases nonlinearly as a function of the increase in Y.

The fastest changes in the ratio ν_{a1}/ν in relation to changes in Y occur for Y=0, i.e., at the beginning of the reset state, and then the rate of these changes decreases as Y increases.

Conclusions

To summarize, on the basis of the Maxwell-Wagner and *JMAK* models, the conductivity parameters of the amorphous part (conductivity and its drift) of a composite consisting of *GST* crystallites immersed in the *GST* amorphous matrix, were identified at which the results of

conductivity drift measurements of this composite in the reset state are met. As a result of the crystallization process, the conductivity of the remaining amorphous phase fraction decreases further compared to that predicted by expressions (1,2), i.e., from the energetic point of view, it goes further into the perfect glassy state, e.g., according to the mechanical strain relief model [4,12,13].

The assumption underlying the interpretation of the conductivity measurements in the reset state with respect to the conductivity drift exponent, which identifies the measured conductivity drift exponent of the composite ν with that of the amorphous fraction of this composite ν_{a1}, was analysed in relation to the crystallization progress in the reset state.

It has been shown that this assumption proved valid only at the beginning of the reset state, and there is deviation from this assumption for $Y(t)$>0.

The deviations of ν_{a1} from ν increase with the increase of Y and n, and this increase is significant, e.g., within the considered $JMAK$ and Maxwell-Wagner models and increments of Y from 0 to 0.3 and n from 0 to 5, the ratio ν_{a1}/ν increases from 1 to 21.29. The rate of this increase decreases as Y increases and increases linearly as n increases.

Thus, conductivity drift models based on the theory of conductivity in amorphous GST and conductivity drift values determined for the composition consisting of GST crystallites immersed in an amorphous GST matrix, may, therefore, lead to erroneous conclusions about the drift's origins, these deepening with the increase of Y.

Acknowledgements: *This work was supported by the Military University of Technology Research Grant under Grant Number 724.*

Author: *dr hab.inż. Kazimierz J. Pluciński, Wojskowa Akademia Techniczna, Wydział Elektroniki, ul, Kaliskiego 2, 00-908 Warszawa, E-mail: kazimierz.plucinski@wat.edu.pl*

REFERENCES

[1] Le Gallo M. and Sebastian A., Topical Review: An overview of phase-change memory device physics, *J. Phys. D Appl. Phys.,* 53 (2020), No. 21, 213002 (27 pp)

[2] Redaelli A., Editor, "*Phase Change Memory - Device Physics, Reliability and Applications*", Ch. 2: Ielmini D., "*Electrical Transport in Crystalline and Amorphous Chalcogenide"*; Ch.5: Gleixner R., "*PCM Main Reliability Features",* (New York: Springer - 2018)

[3] Ielmini D., Lavizzari S., Sharma D., and Lacaita A.L., Physical interpretation, modeling and impact on phase change memory (PCM) reliability of resistance drift due to chalcogenide structural relaxation, *Tech. Dig. – Int. Electron Devices Meet.*, 939-942 (IEDM-2007)

[4] Im J., Cho E., Kim D., Horii H., Ihm J., Han S., A microscopic model for resistance drift in amorphous $Ge_2Sb_2Te_5$, *Curr.Appl.Phys*., 11(2011), No. 2-sup, e82-e84

[5] Zhang W. and Ma E., Unveiling the structural origin to control resistance drift in phase-change memory materials, *Materials Today,* 41 (2020), No. Dec.,156-176

[6] Boniardi M., Redaelli A., Pirovano A., Tortorelli I., Ielmini D., and Pellizzer F., A physics-based model of electrical conduction decrease with time in amorphous $Ge_2Sb_2Te_5$, *J. Appl. Phys*., 105 (2009),No. 8, 084506(5 pp)

[7] Noé P. et al., Phase-change materials for non-volatile memory devices: from technological challenges to materials science issues, *Semicond. Sci. Technol.,* 33 (2018), No. 1, 013002(32 pp)

[8] Sebastian A., Le Gallo M., Burr G.W., Kim S., BrightSky M., and Eleftheriou E., Tutorial: Brain-inspired computing using phase-change memory devices, *J. Appl. Phys*., 124 (2018), No.11, 111101(1)-111101(15)

[9] Zhang W., Mazzarello R, Wuttig M. and Ma E., Designing crystallization in phase-change materials for universal memory and neuro-inspired computing, *Nat. Rev. Mater.,* 4 (2019), No. 3, 150-168

[10] Le Gallo M., Krebs D., Zipoli F., Salinga M., and Sebastian A., Collective Structural Relaxation in Phase-Change Memory Devices, *Adv. Electron. Mater*., 4 (2018), No. 9, 1700627(13 pp)

[11] Elliott S.R., Electronic mechanism for resistance drift in phase change memory materials: link to persistent photoconductivity, *J. Phys. D Appl. Phys*., 53(2020), No. 21, 214002 (7 pp)

[12] Im J., Cho E., Kim D., Horii H., Ihm J. and Han S., Effects of pressure on atomic and electronic structure and crystallization dynamics of amorphous $Ge_2Sb_2Te_5$, *Phys. Rev.,* B 81 (2010), No. 24, 245211(5 pp)

[13] Karpov I.V. et al., Fundamental drift of parameters in chalcogenide phase change memory, *J. Appl. Phys*., 102(2007), No. 12, 124503(6 pp)

[14] Fantini P., Brazzelli S., Cazzini E., and Mani A., Band gap widening with time induced by structural relaxation in amorphous $Ge_2Sb_2Te_5$ films, *Appl. Phys. Lett.,* 100 (2012), No. 1, 013505(4 pp)

[15] Bruggeman D.A.G., Berechnung verschiedener physikalischer Constanten von heterogenen Substanzen, *Ann. Phys*., 416 (1935), No. 7, 636-664

[16] Macdonald J.R., Editor, "*Impedance Spectroscopy*", Wiley, New York, 1987

[17] Gonzalez-Hernandez J.et al., Amorphous-to-crystalline phase transition, J. Vac. Sci. Technol., A 19 (2001), No. 4, 1623-1629

[18] Senkader S. and Wright C.D., Models for phase-change of $Ge_2Sb_2Te_5$ in optical and electrical memory devices, *J. Appl. Phys*., 95 (2004), No. 2, 504-511

[19] Blanc W. et al., The past, present and future of photonic glasses: A review in homage to the United Nations International Year of glass 2022, *Progress in Materials Science,* 134 (2023), No. April, 101084(70 pp)

[20] Jin O., Shang Y, Huang X, Szabó D.V., Le T.T., Wagner S, Klassen T, Kübel Ch., Pistidda C, and Pundt A, Transformation Kinetics of $LiBH_4$–MgH_2 for Hydrogen Storage, *Molecules,* 27 (2022), No. 20, 7005 (15 pp)

[21] Blázquez J.S., Romero F.J., Conde C.F, and Conde A., A Review of Different Models Derived from Classical Kolmogorov, Johnson and Mehl, and Avrami (KJMA) Theory to Recover Physical Meaning in Solid-State Transformations, *Phys. Status Solidi B,* 259 (2022), No. 6, 2100524(21 pp)

[22] Redaelli A., Editor, "*Phase Change Memory - Device Physics, Reliability and Applications"* Ch. 4: A. Redaelli "*Self-Consistent Numerical Model*" (New York: Springer - 2018)

[23] Ielmini D. and Boniardi M., Common signature of many-body thermal excitation in structural relaxation and crystallization of chalcogenide glasses, *Appl. Phys. Lett*., 94 (2009), No. 9, 091906(3 pp)

[24] Russo U., Ielmini D., Redaelli A., and Lacaita A.L., Intrinsic data retention in nanoscaled phase-change memories - Part I: Monte Carlo model for crystallization and percolation, *IEEE Trans. Electron Dev*., 53(2006), No.12, 3032-3039

[25] Russo U., Ielmini D., and Lacaita A.L., Analytical modeling of chalcogenide crystallization for PCM data-retention extrapolation, *IEEE Trans. Electron Dev*., 54(2007), No.10, 2769-2777